THE JOURNAL OF PHYSICAL CHEMISTRY B

ARTICLE

pubs.acs.org/JPCB

Giant Pumping of Single-File Water Molecules in a Carbon Nanotube

Y. Wang,*,† Y. J. Zhao,*,‡ and J. P. Huang*,†

†Department of Physics and State Key Laboratory of Surface Physics, Fudan University, Shanghai 200433, China

‡Advanced Materials Laboratory, Fudan University, Shanghai 200438, China

ABSTRACT: Achieving a fast, unidirectional flow of single-file water molecules (UFSWM) across nanochannels is important for membrane-based water purification or seawater desalination. For this purpose, electro-osmosis methods are recognized as a very promising approach and have been extensively discussed in the literature. Utilizing molecular dynamics simulations, here we propose a design for pumping water molecules in a single-walled carbon nanotube in the presence of a linearly gradient electric (GE) field. Such a GE field is inspired by GE fields generated from charged ions located adjacent to biological membrane water nanochannels that can conduct water in and out of cells and can be experimentally achieved by using the charged tip of an atomic force microscope.

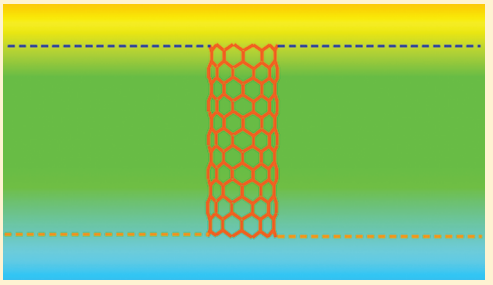

As a result, the maximum speed of the UFSWM can be 1 or 2 orders of magnitude larger than that in a uniform electric (UE) field. Also, inverse transportation of water molecules does not exist in case of the GE field but can appear for the UE field. Thus, the GE field yields a much more efficient UFSWM than the UE field. The giant pumping ability as revealed is attributed to the nonzero net electrostatic force acting on each water molecule confined in the nanotube. These observations have significance for the design of nanoscale devices for readily achieving controllable UFSWM at high speed.

INTRODUCTION

In nature, the transportation of water molecules across water nanochannels in membranes plays an important role in biological activities.[1−3] Water permeation through membranes can be regulated by pH,[4,5] solute concentration,[6,7] and temperature.[8,9] Inspired by the biological implications, people also manipulate the flow of water molecules across nanochannels, to realize abundant applications.[10−14] One of the applications corresponding to unidirectional flow of single-file water molecules (UFSWM) in nanochannels is membrane-based water purification or seawater desalination,[10] where nanochannels located in the membrane should have a diameter small enough so that only water molecules are allowed to enter while other particles larger than a water molecule cannot move in. As a result, progress in this direction has been made by designing systems with an osmotic or hydrostatic pressure gradient (System I),[10] with an imbalance of surface tension (System II),[15] with a chemical[16] or thermal gradient[17] (System III), or with external electric fields or charges (System IV).[18−21] However, for System I, one has to add a large reservoir of solution on one side of the nanochannel to produce the pressure gradient, which is practically difficult. On the other hand, it is also difficult for Systems II or III to yield a controllable UFSWM. The methods for achieving System IV are called "electro-osmosis methods", which are recognized as a very promising approach because they can be readily used to realize controllable UFSWM. However, it is still up to now a challenge to get a fast UFSWM through electro-osmosis methods because a slow UFSWM makes the above-mentioned application impossible or far from being satisfactory.

It has been well recognized that a single-walled carbon nanotube (SWCNT) can be used as a model system to exploit some of the primary behavior of biological membrane water nanochannels that can conduct water in and out of cells.[18−28] Furthermore, controlling UFSWM across SWCNTs also has very great significance for applications like the desalination of seawater.[10] A water molecule is noncharged as a whole but possesses a plentiful quantity of electric charges: charge quantity on the oxygen atom is $-0.834e$ (e: the elementary charge, 1.6×10^{-19} C); charge quantity on a hydrogen atom is $0.417e$.[29] Thus, recently some novel explorations utilized electro-osmosis methods to realize UFSWM across SWCNTs by applying external charges or electric fields,[18−21] which can electrostatically interact with water molecules. On the basis of molecular dynamics simulations, Gong et al.[18] reported that water molecules can be caused to unidirectionally transport across a (6, 6) SWCNT (with length 2.3 nm) by putting three point charges on the surface of a SWCNT, which produce a biased potential to allow water permeation across the SWCNT: the maximum speed of the UFSWM is 4.4 ns^{-1}. Later, this method was reperformed and showed a lower speed.[19] On the other hand, Joseph et al.[20] applied a uniform electric (UE) field along a SWCNT axis to drive water molecules within a (10, 0) SWCNT (with length 9.83 nm), and the UFSWM with maximum speed 8.1 ns^{-1} was also shown to appear along the orientation of water molecules. Then, Su et al.[21] systematically investigated the transport of single-file water molecules through a (6, 6) SWCNT (with length 1.34 nm) in a UE field. They also found UFSWM (with maximum speed 1.2 ns^{-1}) along the orientation of water

Received: July 21, 2011
Revised: September 30, 2011
Published: October 06, 2011

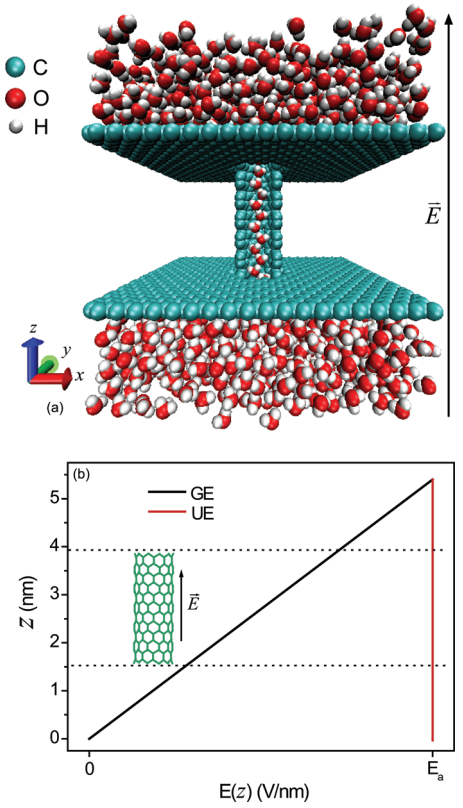

Figure 1. (a) Introduction to the simulation box. Two parallel fixed graphite sheets with separation 2.380 nm divide the box [with dimensions $L_x \times L_y \times L_z = 4.650\ \text{nm} \times 4.650\ \text{nm} \times 5.434\ \text{nm}$] into three parts. A z-directed, uncapped, semiconducting (10, 0) SWCNT with diameter 0.772 nm and length 2.38 nm perpendicularly joins the two graphite sheets. The box contains 1826 water molecules; within the area between the two graphite sheets, there are no water molecules outside the SWCNT. The bottom of the simulation box is located at $z = 0$, and the two ends of the SWCNT are located at $z = 1.527$ and 3.907 nm, respectively. The box is subjected to a UE or GE field, $\vec{E}$, directed along the z-axis. (b) The strengths of the UE and GE field are given by $E = E_a$ and $E = E_a(z/L_z)$, respectively. Here $0 \le z \le L_z$ and $0 \le E_a \le 8$ V/nm.

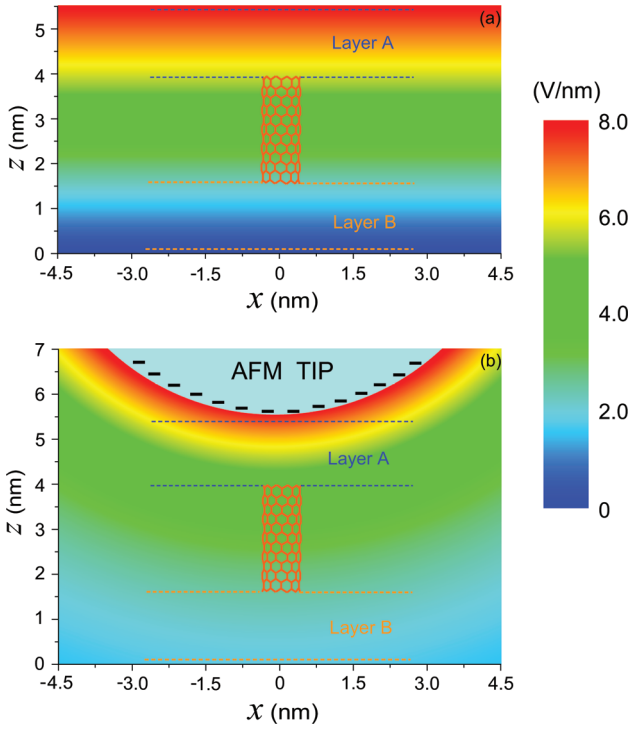

Figure 2. Spatial distribution of the strengths of two GE fields according to the finite element method.[32] One is (a) a GE field, E, according to $E = E_a(z/L_z)$ with $E_a = 8.0$ V/nm, which, for the sake of generality, is adopted for our simulations, and the other is (b) a GE field generating from a charged tip of an AFM (detailed parameters can be found in the text), which shows an experimental method for approximately generating such a GE field as that in (a).

molecules confined in the SWCNT. It was revealed that, when the orientation of the water molecules is maintained along one direction due to an external electric field, the UFSWM along that direction can be attained due to coupling between rotational and translational motions.[20]

Utilizing molecular dynamics simulations, here we propose a design for achieving giant pumping of water molecules in a (10, 0) SWCNT with length 2.38 nm in the presence of a linear GE field [Figure 1(b) or Figure 2(a)]. The use of such a GE field is inspired by ions located adjacent to biological membrane water nanochannels. Such ions come to appear due to ionization of membrane proteins, and each of them is charged, thus generating a GE field covering the nanochannels. On the other hand, in experiments, the GE field of interest can be achieved by using the charged tip of an atomic force microscope (AFM) [Figure 2(b)].[30,31] To this end, we find that the speed of the UFSWM in such a GE field is generally 1 or 2 orders of magnitude larger than that in a UE field. In the mean time, inverse transportation of water molecules does not exist in the case of the GE field but can appear for the UE field. Thus, we conclude that the GE field yields a much more efficient UFSWM than the UE field. The giant pumping ability is attributed to the nonzero net electrostatic force acting on each water molecule confined in the SWCNT subjected to the GE field. These results have significance for the design of nanoscale devices for readily achieving controllable UFSWM at high speed.

METHODOLOGY

Molecular dynamics, which has been widely used for the study of water dynamics in SWCNTs,[18−28] is adopted herein. Our simulation framework is shown in Figure 1(a). The force field parameters of the SWCNT come from Hummer et al.,[22] and the TIP3P water model is applied.[29] For simulations, we choose a linear GE field [as shown in Figure 1(b) and Figure 2(a)]. The simulation box shown in Figure 1(a) has also been displayed in Figure 2(a) where the distribution of the linear GE field is given according to the finite element method.[32] In Figure 2(a), layers A and B denote water containers, which are joined by the SWCNT. Without loss of generality, a linear GE field is adopted for our simulations. For comparison, we also use a uniform electric (UE) field. As shown in Figure 1(b), the strengths of the UE field and GE field are, respectively, given by $E = E_a$ and $E = E_a(z/L_z)$. Clearly, the parameter set insures that the strength of the GE field does not exceed that of the UE field at any z ($0 \le z < L_z$). Here L_z is defined in the caption of Figure 1(a), $L_z = 5.434$ nm, and E_a is an adjustable parameter, $0 < E_a < 8.0$ V/nm. Throughout this work, E_a is set to be smaller than the experimental value, 28.2 V/nm, adopted by Tony et al.[33] when they used in situ X-ray

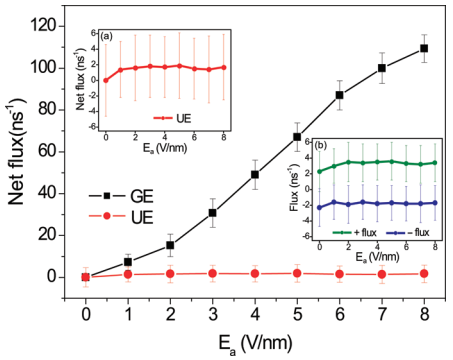

Figure 3. Net flux (= "+ flux" − "− flux") of water molecules transporting across the SWCNT in the GE or UE fields. Here, "+ flux" and "− flux" denote the number of water molecules per nanosecond transferring across the SWCNT along the + z and − z axis, respectively. Specifically, "− flux" is always zero for the GE fields. For clarity, inset (a) shows the net flux in the UE field only, which just corresponds to the "+ flux" and "− flux" displayed in inset (b).

scattering to measure the water density profile perpendicular to a Ag(111) surface. On the other hand, we have also done some theoretical analysis. Details: Because the bond energy of HO^-, W, is W = 463 kJ/mol, the upper limit of an electric field, E_L, acting upon one water molecule can be estimated as about E_L = 12.0 V/nm according to the relation $qE_LD = W/N_A$, where D = 0.4 nm is the dimension of a water molecule, q the charge quantity of H^+, $q = e$, and N_A Avogadro's constant. It is worth noting that this is a very rough theoretical estimation because we do not take into account interactions between molecules. Certainly, if we use a larger E_a, E_a > 8.0 V/nm, the pumping ability due to GE fields can be enhanced accordingly. All simulations are carried out in the NVT ensemble at a constant temperature of 300 K, by using the velocity rescaling thermostat[34] on the basis of the molecular dynamics package Gromacs 4.0.5. Periodic boundary conditions are applied in the simulations. The van der Waals interactions are calculated with a cutoff (1.4 nm). The particle-mesh Ewald method is used to treat the long-rang electrostatic interactions.[35] All simulations are run for 155 ns, and the last 150 ns are used for data analysis. A time step of 2.0 fs is used, and data are collected every 1.0 ps.

Regarding the GE field under our consideration, more comments should be added. For the sake of generality, the GE field shown in Figure 1(b) or Figure 2(a) is used for simulations, which can be experimentally obtained by using some particular methods. For instance, one may resort to an AFM tip located above Layer A as shown in Figure 2(b). The apex of an AFM tip is often spherical with a certain radius,[31] R, and electric charges can be congregated on the tip.[30,31] In AFM experiments, the electric field near the apex of the charged tip can attain the strength with the order of magnitude, 1 V/nm.[30] For Figure 2(b), we choose R = 5.0 nm, which is available in experiments. Then, we assume that negative charges with electric charge quantity, 140e, are included in this apex. The distribution of the electric field is computed according to the finite element method.[32] As a result, a GE field with strength from 0 to 8.0 V/nm is formed along the direction of the SWCNT (see Figure 2(b)). In other words, the general linear GE field [Figure 1(b) or Figure 2(a)] used for our simulations can be approximately generated by a charged AFM tip [Figure 2(b)].

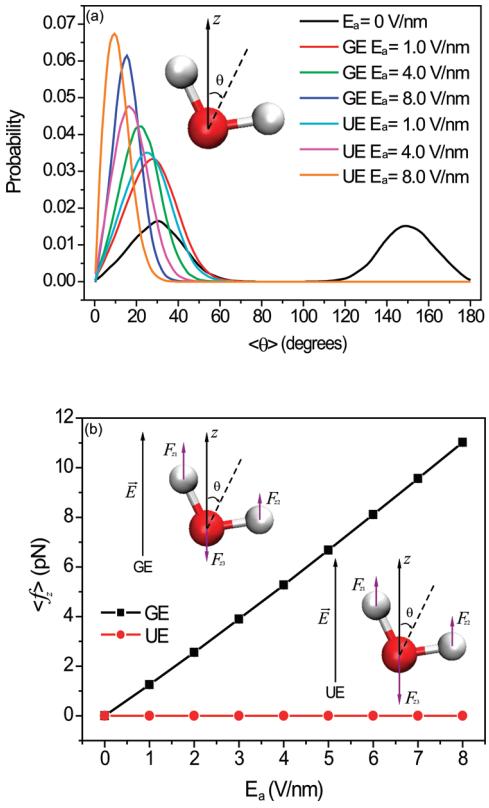

Figure 4. (a) Probability distribution of the averaged angle, $\langle\theta\rangle$, of the water molecules inside the SWCNT for zero field (E_a = 0 V/nm) and various UE or GE fields. As shown in the inset, here θ is the angle between a water molecule (seen as a dipole) and z-axis, and $\langle\cdots\rangle$ denotes the average over all the water molecules inside the SWCNT. For convenience, 0° < $\langle\theta\rangle$ <90° and 90° < $\langle\theta\rangle$ <180° denote the "+ dipole" and "− dipole" states of the water molecules inside the SWCNT, respectively. As shown in (a), only the "+ dipole" state appears for either GE or UE fields. (b) The averaged net electrostatic force, $\langle f_z\rangle$, acting on a water molecule within the SWCNT as a function of E_a in the GE or UE fields. Clearly, $\langle f_z\rangle$ is nonzero for the GE fields (with E_a > 0 V/nm) and increases as E_a increases. However, $\langle f_z\rangle$ is always zero for the UE fields. This can be understood according to the two insets: (left inset) for a water molecule in the GE field, the electrostatic forces acting on one oxygen atom and two hydrogen atoms always satisfy $F_{z1} + F_{z2} > F_{z3}$ [due to the "+ dipole" state of the water molecule as shown in (a)], thus yielding a nonzero net force, $f_z = F_{z1} + F_{z2} - F_{z3} > 0$; (right inset) for a water molecule in the UE field, the electrostatic forces satisfy $F_{z1} + F_{z2} = F_{z3}$, thus yielding a zero net force, $f_z = F_{z1} + F_{z2} - F_{z3} = 0$.

RESULTS AND DISCUSSION

Now we are in a position to discuss the UFSWM across the SWCNT by investigating the net flux of the water molecules in the presence of either GE or UE fields (see Figure 3). First, in the absence of electric fields, no obvious net flux is obtained, which echoes with the report by Wan et al.[24] This also confirms the suitability of the time period, 150 ns, used for data analysis, at least to some extent. Second, in the case of the UE fields, for various E_a's, both "+ flux" and "− flux" occur, and the net flux always maintains the small values ranging from 1.4 to 1.9 water molecules per nanosecond (ns^{-1}). Third, for the GE fields, "− flux" does not exist, and only "+ flux" comes to appear. On the other hand, the net flux increases significantly as E_a increases (see Figure 3). As a result, the maximum speed of the net flux

dx.doi.org/10.1021/jp2069557 |J. Phys. Chem. B 2011, 115, 13275–13279

reaches 109.2 ns^{-1} at E_a = 8.0 V/nm, which is 2 orders of magnitude larger than that of the UE field with E_a = 8.0 V/nm. So we may conclude that the GE fields can yield a much more efficient UFSWM across a SWCNT than the UE fields.

Next, we plot Figure 4 to help reveal the physical mechanism underlying the above results obtained from Figure 3.

Figure 4(a) shows the probability distributions of the averaged angle $\langle\theta\rangle$ of water molecules inside the SWCNT for different kinds of electric fields. The notations have been indicated in the caption. For E_a = 0 V/nm, the two symmetric peaks with respect to $\langle\theta\rangle$ = 90° are clearly shown. That is, we observe the equal probability of "+ dipole" (0° < $\langle\theta\rangle$ <90°) and "− dipole" (90° < $\langle\theta\rangle$ < 180°) states of water molecules when E_a = 0 V/nm. This can be understood: Owing to thermal fluctuations, single-file water molecules flip during the transportation through a nanochannel, yielding a random probability of "+dipole" and "−dipole". On the other hand, even if no electric field is applied, water molecules can also transport across the SWCNT.[24] However, the net flux statistically tends to zero due to the interactions between water molecules, water molecular thermal movements, and so on, accompanying the equal probability of "+ dipole" and "− dipole" states of water molecules,[24] as also shown in Figure 3. More importantly, when GE or UE fields are applied, the "+ dipole" state of water molecules inside the SWCNT always comes to appear, and no "− dipole" state occurs (see Figure 4(a)). This is because each water molecule tends to stay at the most stable state by trying to orientate itself along the z direction to maintain the lowest value of electric energy given by $-\vec{p}\cdot\vec{E}$ in the presence of z-directed UE or GE fields, $\vec{E}$'s. Here, $\vec{p}$ denotes the dipole moment of a water molecule. Accordingly, in such cases, the "− dipole" state of water molecules cannot occur in the SWCNT. It is worth noting that, during the orientation, besides the external electric fields, the water molecules inside the SWCNT are also unavoidably affected by nearby water molecules and by thermal fluctuation, which is the reason why $\langle\theta\rangle$ always deviates from 0°. Additionally, we also find that the locations of peaks move to smaller $\langle\theta\rangle$'s as E_a increases for either GE or UE fields. Furthermore, for a fixed E_a, the peak location of the UE field corresponds to a smaller $\langle\theta\rangle$ than that of the GE field. One can also understand both of the results by resorting to the above analysis, which is based on the electrodynamics requirement for minimizing the electric energy, $-\vec{p}\cdot\vec{E}$, and the influences of nearby water molecules and thermal fluctuation.

Figure 4(b) shows the averaged net electrostatic force, $\langle f_z\rangle$, acting on a water molecule within the SWCNT as a function of E_a in the GE or UE fields. According to this figure (detailed notations have been introduced in the caption), the averaged net electrostatic force $\langle f_z\rangle$ is always nonzero for the GE fields (with $E_a > 0$) due to $f_z = F_{z1} + F_{z2} - F_{z3} > 0$ as shown in the left inset and also increases as E_a increases. However, $\langle f_z\rangle$ is always zero in the presence of UE fields, due to $f_z = F_{z1} + F_{z2} - F_{z3} = 0$ as shown in the right inset. Clearly, this figure reveals the unique mechanism underlying the results obtained from Figure 3, namely, the giant pumping ability and the disappearance of "− flux" in the presence of the GE fields. In a word, for GE fields, the net flux shown in Figure 3 can be seen as a result of the joint effects of both the unidirectional orientations and the GE fields. Reasons are as follows. The unidirectional orientations of water molecules appear naturally due to the orientating ability of the GE field, and then each water molecule in the presence of the GE field is exerted on a nonzero net force (see Figure 4) which drives the molecule to move.

CONCLUSION

On the basis of molecular dynamics simulations, we have investigated a UFSWM across a (10, 0) SWCNT subjected to a GE or UE field. It has been found that the maximum speed of the UFSWM in the GE field can be 1 or 2 orders of magnitude larger than that in the UE field. Meanwhile, inverse transportation of water molecules does not exist in the presence of the GE field but can appear for the UE field. Therefore, the GE field yields a much more efficient UFSWM than the UE field. It is revealed that the giant pumping ability is attributed to the interaction between the GE field and water molecules confined in the nanochannel, which causes an imbalance of forces acting on two hydrogen atoms and one oxygen atom of a water molecule and thus yields a nonzero net electrostatic force on the water molecule. The net force is unidirectional due to the fixed GE field, thus yielding no inverse transportation of water molecules. For experimental demonstration, we also suggest that the GE field can be achieved near the charged AFM tip. This work is relevant for designing nanoscale devices for readily achieving controllable UFSWM at high speed.

AUTHOR INFORMATION

Corresponding Author

*E-mail: wangyuchina@126.com (Y.W.); zhaoyanjiao@fudan.edu.cn (Y.J.Z.); jphuang@fudan.edu.cn (J.P.H).

ACKNOWLEDGMENT

We acknowledge the financial support by the National Natural Science Foundation of China under Grant Nos. 10874025 and 11075035 and by the Chinese National Key Basic Research Special Fund under Grant No. 2011CB922004.

REFERENCES

(1) Murata, K.; Mitsuoka, K.; Hirai, T.; Walz, T.; Agre, P.; Heymann, J. B.; Engel, A.; Fujiyoshi, Y. *Nature* **2000**, *407*, 599–605.
(2) Sui, H. X.; Han, B. G.; Lee, J. K.; Walian, P.; Jap, B. K. *Nature* **2001**, *414*, 872–878.
(3) de Groot, B. L.; Grubm%ller, H. *Science* **2001**, *294*, 2353–2357.
(4) Iwata, H.; Matsuda, T. *J. Membr. Sci.* **1988**, *38*, 185–199.
(5) Ito, Y.; Park, Y. S.; Imanishi, Y. *Langmuir* **2000**, *16*, 5376–5381.
(6) Osada, Y.; Honda, K.; Ohta, M. *J. Membr. Sci.* **1986**, *27*, 327–338.
(7) Yoshimi, Y.; Arai, R.; Nakayama, S. *Anal. Chim. Acta* **2010**, *682*, 110–116.
(8) Yang, M.; Xie, R.; Wang, J. Y.; Ju, X. J.; Yang, L. H.; Chu, L. Y. *J. Membr. Sci.* **2010**, *355*, 142–150.
(9) Lee, S. H.; Chung, G. C.; Steudle, E. *Plant. Cell. Environ.* **2005**, *28*, 1191–1202.
(10) Service, R. F. *Science* **2006**, *313*, 1088–1090.
(11) Majumder, M.; Chopra, N.; Andrews, R.; Hinds, B. *Nature* **2005**, *438*, 44.
(12) Holt, J. K.; Park, H. G.; Wang, Y. M.; Stadermann, M.; Artyukhin, A. B.; Grigoropoulos, C. P.; Noy, A.; Bakajin, O. *Science* **2006**, *312*, 1034–1037.
(13) Ghosh, S.; Sood, A. K.; Kumar, N. *Science* **2003**, *299*, 1042–1044.
(14) Kumar, M.; Grzelakowski, M.; Zilles, J.; Clark, M.; Meier, W. *Proc. Natl Acad. Sci. U.S.A.* **2007**, *104*, 20719–20724.
(15) de Gennes, P. G.; Brochard-Wyart, F.; Quere, D. *Capillarity and Wetting Phenomena*; Springer: New York, 2003.
(16) Chaudhury, M. K.; Whitesides, G. M. *Science* **1992**, *256*, 1539–1541.

(17) Linke, H.; Alemán, B. J.; Melling, L. D.; Taormina, M. J.; Francis, M. J.; Dow-Hygelund, C. C.; Narayanan, V.; Taylor, R. P.; Stout, A. *Phys. Rev. Lett.* **2006**, *96*, 154502(1–4).
(18) Gong, X. J.; Li, J. Y.; Lu, H. J.; Wan, R. Z.; Li, J. C.; Hu, J.; Fang, H. P. *Nat. Nanotechnol.* **2007**, *2*, 709–712.
(19) Wong-ekkabut, J.; Miettinen, M. S.; Dias, C.; Karttunen, M. *Nat. Nanotechnol.* **2010**, *5*, 555–557.
(20) Joseph, S.; Aluru, N. R. *Phys. Rev. Lett.* **2008**, *101*, 064502(1–4).
(21) Su, J. Y.; Guo, H. X. *ACS Nano* **2011**, *5*, 351–359.
(22) Hummer, G.; Rasaiah, J. C.; Noworyta, J. P. *Nature* **2001**, *414*, 188–190.
(23) Li, J. Y.; Gong, X. J.; Lu, H. J.; Li, D.; Fang, H. P.; Zhou, R. H. *Proc. Natl. Acad. Sci. U.S.A.* **2007**, *104*, 3687–3692.
(24) Wan, R.; Lu, H.; Li, J.; Bao, J.; Hu, J.; Fang, H. *Phys. Chem. Chem. Phys.* **2009**, *11*, 9898–9902.
(25) Koga, K.; Gao, G. T.; Tanaka, H.; Zeng, X. C. *Nature* **2001**, *412*, 802–805.
(26) Meng, X. W.; Wang, Y.; Zhao, Y. J.; Huang, J. P. *J. Phys. Chem. B* **2011**, *115*, 4768–4773.
(27) Corry, B. J. *J. Phys. Chem. B* **2008**, *112*, 1427–1434.
(28) Walther, J. H.; Jaffe, R.; Halicioglu, T.; Koumoutsakos, P. *J. Phys. Chem. B* **2001**, *105*, 9980–9987.
(29) Jorgensen, W. L.; Chandrasekhar, J.; Madura, J. D.; Impey, R. W.; Klein, M. L. *J. Chem. Phys.* **1983**, *79*, 926–935.
(30) Agronin, A.; Rosenwaks, Y.; Rosenman, G. *Appl. Phys. Lett.* **2004**, *85*, 452–454.
(31) Ramirez-Aguilar, K. A.; Rowlen, K. L. *Langmuir* **1998**, *14*, 2562–2566.
(32) Gao, Y.; Huang, J. P.; Liu, Y. M.; Gao, L.; Yu, K. W.; Zhang, X. *Phys. Rev. Lett.* **2010**, *104*, 034501(1–4).
(33) Toney, M. F.; Howard, J. H.; Richer, J.; Borges, G. L.; Wiesler, D. G.; Yee, D.; Sorensen, L. B. *Nature* **1994**, *368*, 444–446.
(34) Bussi, G.; Donadio, D.; Parrinello, M. *J. Chem. Phys.* **2007**, *126*, 014101(1–7).
(35) Darden, T. A.; York, D. M.; Pedersen, L. G. *J. Chem. Phys.* **1993**, *98*, 10089(1–4).